International Journal of Minerals, Metallurgy and Materials
Volume 20, Number 3, March 2013, Page 259
DOI: 10.1007/s12613-013-0721-8

Effects of aging treatment and heat input on the microstructures and mechanical properties of TIG-welded 6061-T6 alloy joints

Dong Peng[1], *Jun Shen*[1], *Qin Tang*[1], *Cui-ping Wu*[1], *and Yan-bing Zhou*[2]

1) College of Material Science & Engineering, Chongqing University, Chongqing 400044, China
2) Fabrication Workshop, Dongfang Turbine Co., Ltd., Deyang 618000, China
(Received: 7 May 2012; revised: 9 June 2012; accepted: 12 June 2012)

Abstract: Aging treatment and various heat input conditions were adopted to investigate the microstructural evolution and mechanical properties of TIG welded 6061-T6 alloy joints by microstructural observations, microhardness tests, and tensile tests. With an increase in heat input, the width of the heat-affected zone (HAZ) increases and grains in the fusion zone (FZ) coarsen. Moreover, the hardness of the HAZ decreases, whereas that of the FZ decreases initially and then increases with an increase in heat input. Low heat input results in the low ultimate tensile strength of the welded joints due to the presence of partial penetrations and pores in the welded joints. After a simple artificial aging treatment at 175°C for 8 h, the microstructure of the welded joints changes slightly. The mechanical properties of the welded joints enhance significantly after the aging process as few precipitates distribute in the welded seam.

Keywords: aluminum alloys; tungsten inert gas welding; heat input; aging; mechanical properties; microstructure

1. Introduction

The typical aging hardening aluminum alloy 6061-T6 is widely used in automotives, ships, and electronics industries because of its medium strength, good formability, and corrosion resistance [1]. In modern industry, welding is one of the most used methods for joining aluminum and its alloys [2]. The preferred welding process for these alloys is frequently tungsten inert gas (TIG) welding due to its comparatively easier applicability and better economy [3].

Almost all heat-treatable aluminum alloys are prone to softening and hot cracking after arc welding. Recently, a simple and effective treatment (post-weld aging treatment) has been adopted to improve the mechanical properties of welded aluminum alloy joints. Temmar *et al.* [4] studied the effect of post-weld aging treatment on the mechanical properties of TIG-welded low thickness 7075 aluminum alloy joints; they found that the tensile strength, yield strength, and elongation improve significantly after post-weld aging treatment. Balasubramanian *et al.* [5] researched the effect of pulsed current and post-weld aging treatment on the tensile properties of TIG-welded and metal inert gas (MIG)-welded high-strength aluminum alloys; they pointed out that more precipitates are formed during post-weld aging treatment, and their uniform distribution results in a higher strength and hardness. Malarvizhi and Balasubramanian [6] discussed the effects of welding processes and post-weld aging treatment on the fatigue behavior of AA2219 aluminum alloy joints by TIG, electron beam welding, and friction stir welding; they concluded that fatigue strength of the welded joints is enhanced greatly after heat treatment.

The above-mentioned investigations mainly focused on the influence of welding methods on the microstructures and mechanical properties of the artificially aged aluminum alloy-welded joints. However, the influence of the welding parameters (in particular, heat input) and post-weld aging treatment on the microstructures and mechanical properties of the TIG-welded 6061-T6 aluminum alloy joints is still an open question. Hence, in this article, an

Corresponding author: Jun Shen E-mail: shenjun@cqu.edu.cn

attempt has been made to clarify the question presented above. Moreover, the fracture mechanisms of the welded beams were also discussed in detail.

2. Experimental

Commercial 6061-T6 aluminum alloy plates with a dimension of 100 mm × 50 mm × 3 mm were used for the welding tests (provided by Southwest Aluminum (Group) Co., Ltd., China). To avoid the influence of oxides and grease on the plate surfaces, the surfaces of the samples were scratched by a steel brush and then were washed with acetone. Single-pass welding without any filler was used to fabricate square-butt joints. To avoid hot cracking, pores, and distortion, some trial tests were adopted and the final welding parameters are presented in Table 1. Here, the shielding gas (helium), welding voltage, and welding speed were constant. The heat input (L) of welding is determined by

$$L = \eta \frac{UI}{V} \tag{1}$$

Table 1. TIG welding parameters

Samples	Current / A	Voltage / V	Welding speed / $(\mathrm{mm \cdot s^{-1}})$	Heat input / $(\mathrm{J \cdot mm^{-1}})$
A	110	20	10	198
B	120	20	10	216
C	130	20	10	234
D	140	20	10	252
E	150	20	10	270

where U is the welding voltage, V is the welding speed, I is the welding current, and η is the efficiency of TIG welding ($\eta = 0.90$ [7]).

To investigate the influence of post-weld aging treatment on the microstructures and tensile properties of the welded joints, the samples were divided into two groups: (1) as-welded joints and (2) artificially aged joints. The artificial aging was performed at 175°C in an induction furnace for 8 h and then the samples were cooled down to room temperature in the furnace [8].

After welding, the cross-sections of welded joints were prepared by standard metallographic procedures (grinding, polishing, and etching with a solution of 95vol% H_2O + 2.5vol% HNO_3 + 1.5vol% HCl + 1.0 vol% HF for 45-50 s). The microstructures were characterized with an optical microscope (MDJ200). A hardness tester (HXS-1000AY) was used for the microhardness test with a period of 20 s, a load of 4.9 N, and a step size of 0.5 mm. Hardness was measured at numerous points from the weld centerline along the heat-affected zone (HAZ) to the base material (BM) zone. The room temperature tensile tests were carried out on a tensile machine (SANS-XUA305C) with a tensile speed of 1 mm/min. The tensile samples were prepared according to the ISO 6892-1:2009 standard. Three tensile samples cutting from the same joint were tested and the average values were collected to evaluate the weld metal's tensile properties. A scanning electron microscope (SEM; TESCAN, Inc., VegaIILMU SEM) was used for the fractographic examination.

3. Results and discussion

3.1. Typical microstructures of the TIG-welded 6061-T6 aluminum plates

Fig. 1 shows a typical microstructure of the as-welded

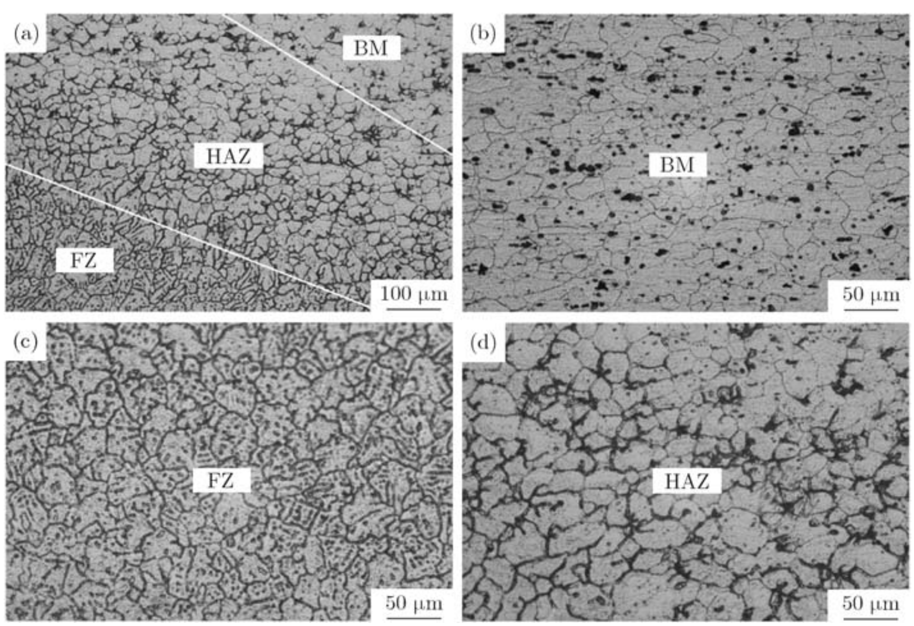

Fig. 1. Typical microstructure images of 6061-T6 TIG-welded joints at a heat input of 234 J/mm: (a) whole welded joint zone; (b) BM zone; (c) FZ, (d) HAZ.

joint at a heat input of 234 J/mm. The welded joint is composed of a fusion zone (FZ), a wide HAZ, and a BM area (Fig. 1(a)). Irregular distribution of coarse particles throughout the BM is observed clearly (Fig. 1(b)). These particles are believed to form during casting and subsequent T6 aging treatment [9]. An equiaxed dendritic network is formed in the FZ (Fig. 1(c)). Generally, the fine microstructure of the FZ is attributed to the high cooling rate associated with the TIG welding [10]. Compared with grains in both the FZ and the BM, the grains coarsen markedly in the HAZ (Fig. 1(d)).

3.1.1. Effects of heat input on the microstructures of the TIG-welded joints

Fig. 2 illustrates the microstructural evolution of the as-welded joints with an increase in heat input. The width of the HAZ and the average grain size of the FZ were determined by a quantitative metallographic method [11] and the results are collected in Fig. 3. The width of the HAZ increases from about 335 to 690 μm with an increase in heat input. Low heat input reduces the peak temperature of the molten pool and results in the narrow HAZ (Figs. 2(a) and 2(b)). However, a higher heat input prolongs the solidification process and gives a more heat input to the BM, which results in a wider HAZ (Figs. 2(d) and 2(e)). In addition, the increase in heat input leads to the coarsening of the grains in the FZ (Fig. 3). This is because the increase in heat input provides more driving force for grain boundary migration and then speeds the growth of the grains [12].

3.1.2. Effects of post-weld aging treatment on the microstructures of the TIG-welded joints

Fig. 4 shows the optical micrographs of the as-welded joints and artificially aged joints (L = 252 J/mm). No

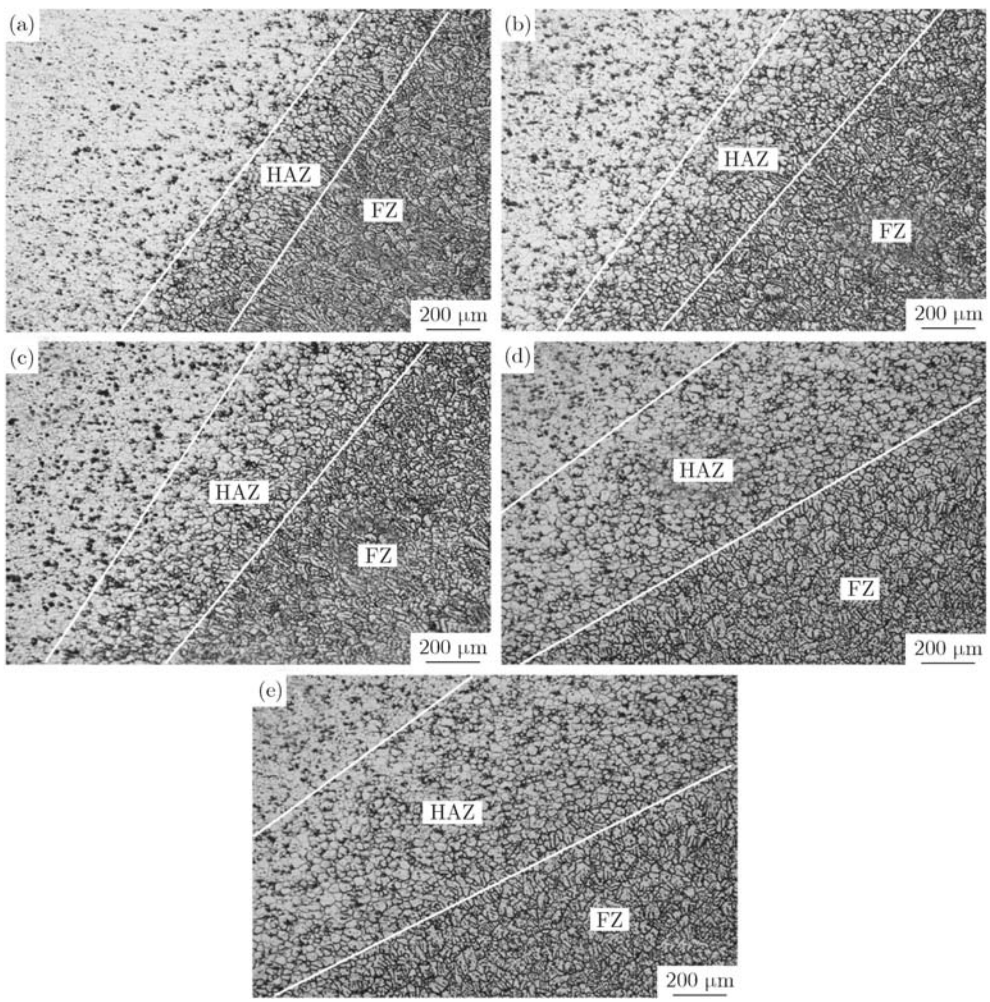

Fig. 2. Optical images of 6061-T6 TIG-welded joints at different heat inputs: (a) 198 J/mm; (b) 216 J/mm; (c) 234 J/mm; (d) 252 J/mm; (e) 270 J/mm.

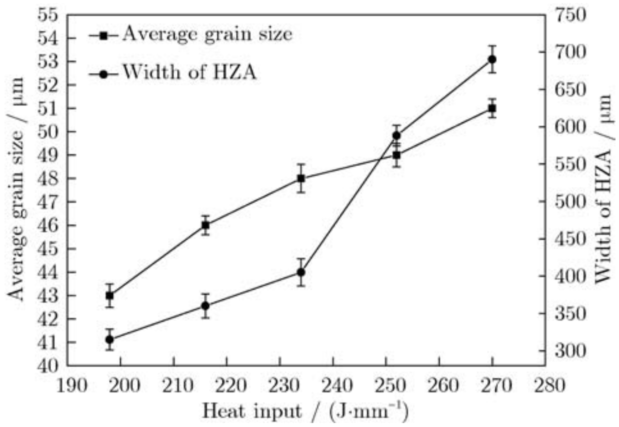

Fig. 3. Effect of heat input on the average grain size of the FZ and the width of the HAZ.

appreciable changes in grain size have been noticed in the aged joins, and this is similar with the results provided by Malarvizhi *et al.* [13]. However, the artificial aging treatment leads to the precipitation strengthening greatly. Generally, in the TIG-welded aluminum alloy joints, the modification of precipitates involves four types of reactions [14]: (1) dissolution of precipitates, (2) growth or transformation of coherent precipitates to incoherent forms, (3) direct formation of coherent precipitates from the solid solution, and (4) direct formation of incoherent precipitates from the solid solution at high temperature. All of these transformations may present in the FZ of the welded 6061-T6 aluminum alloy joints due to re-melting and re-solidification processes. At the end of solidification, the precipitation aging reaction is suppressed by the lack of essential elements because of the formation of eutectic constituents [4]. However, the modification of precipitates in the HAZ is mainly determined by two solid-state reactions [15]: (1) dissolution of precipitates and coarsening grains in the zone submitted to higher peak temperatures (Fig. 4(a)) and (2) transformation of metastable phases to stable phases in the zone submitted to a lower peak temperature. Therefore, when the temperature changes greatly, such as in the welding process, the precipitation state will be modified significantly and this has a great impact on the mechanical behavior of the welded joints.

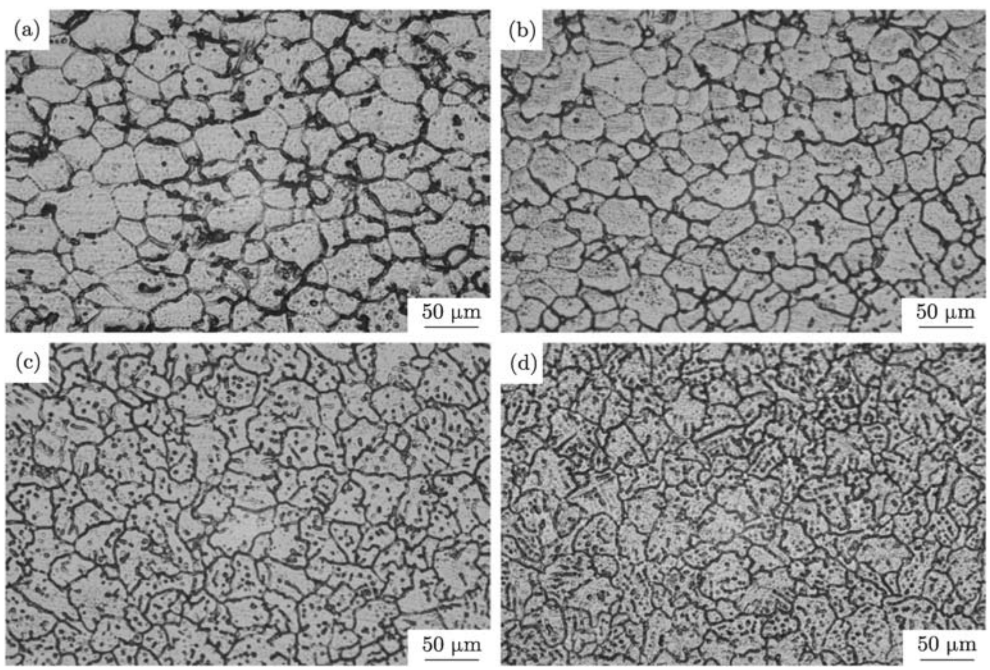

Fig. 4. Optical images of 6061-T6 TIG-welded joints with or without post-weld treatment: (a) HAZ, as-welded; (b) HAZ, artificially aged; (c) FZ, as-welded; (d) FZ, artificially aged.

3.2. Effects of post-weld aging treatment and heat input on the mechanical properties of the TIG-welded joints

3.2.1. Hardness

Fig. 5 shows the microhardness profiles measured along the weld centerline to the BM at the heat input of 234 J/mm. With an increase in the distance from the weld centerline, the hardness values increase gradually. In an aged hardenable aluminum alloy, the hardness is determined by the strengthening precipitate characteristics such as size, morphology, and volume fraction [16]. Moving from the FZ to the BM, the effect on the strengthening precipitates becomes smaller due to thermal cycling in the TIG welding. Therefore, the microhardness relationships among the BM, HAZ, and FZ of welded joints are BM>HAZ>FZ. The hardness values of FZ and HAZ are higher in the artificial aging treatment-welded joints than those of the as-welded joints (Fig. 5) because of the formation of hardening precipitates during the artificial aging treatment.

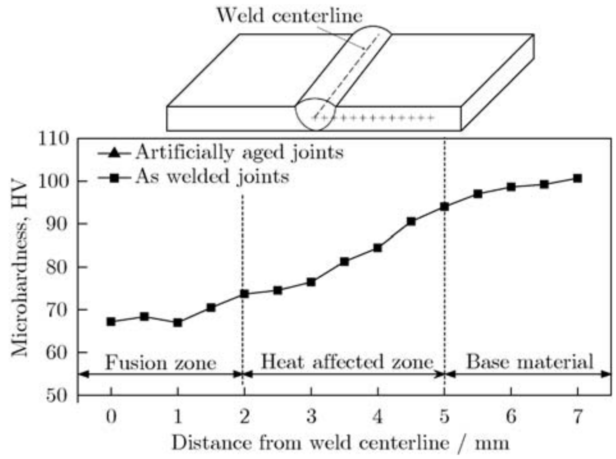

Fig. 5. Typical microhardness profiles across the TIG-welded joints at a heat input of 234 J/mm.

Fig. 6 shows the variations in microhardness values versus different heat inputs. Before post-weld aging treatment, with an increase in heat input, the hardness of the FZ decreases initially and then increases slightly (Fig. 6(a)). The lowest hardness value (HV 67) is achieved at the heat input of 252 J/mm, corresponding to approximately 64% of the BM (HV 105). This is due to the coarsening of grains and the lack of strengthening phases, which resulted by the thermal cycle during the TIG welding process. The grain size plays a dominant role for hardness in this situation [16]. Due to the change in grain size of the FZ (Fig. 3) and the Hall-Petch relationship, the hardness of the FZ decreases with an increase in heat input. However, when the heat input increases over 252 J/mm, the hardness of the FZ increases slightly. This is because the excess heat input reduced the cooling rate of the welded joint and this is conducive to the formation of hardening precipitates, which dominates the hardness of the FZ. After post-weld aging treatment, it is found that the simple aging treatment is beneficial for improving the hardness of the FZ (Fig. 6(a)).

The hardness of the HAZ of the as-welded joints decreases gradually from HV 86 to 76 with the increase in heat input (Fig. 6(b)) and this is because of the modification of precipitates and the change in width of the HAZ (Fig. 2). It is found that the hardness of the HAZ recovers partly after post-weld aging treatment. However, the hardness of the aged joints reduces slightly when the heat input exceeds 252 J/mm (see Fig. 6(b)). This is presumably due to the higher heat input leading to over-aging of the HAZ. This behavior observed here is in agreement with the report by Ma and den Ouden [14] on a 7020 aluminum alloy welding.

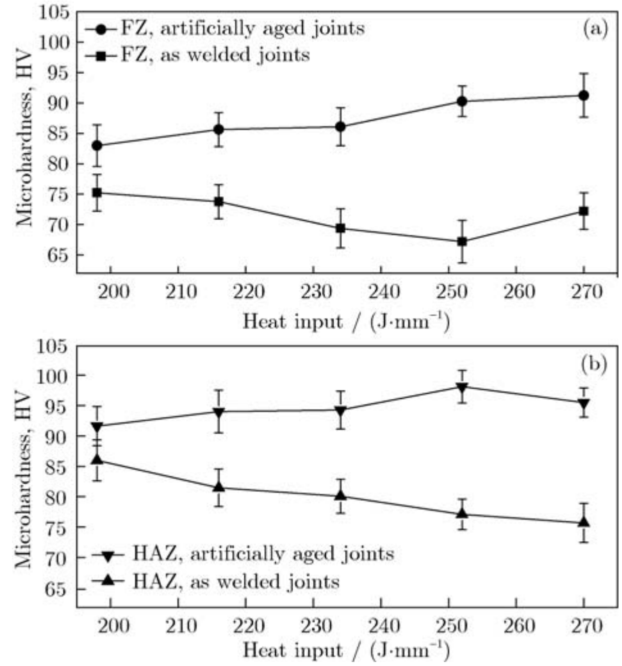

Fig. 6. Microhardness of the FZ (a) and HAZ (b) under various heat input conditions.

3.2.2. Tensile properties

Fig. 7 shows the typical effects of heat input and post-weld aging treatment on the ultimate tensile strength (UTS) values of the TIG-welded 6061-T6 joints. At low heat input (198 J/mm), partial penetrations and pores exist at the limited zone of the as-welded joints (Fig. 7(a)). In this condition, the UTS value is 136.4 MPa, which is only 50% of the BM (272.7 MPa). The shielding gas usually

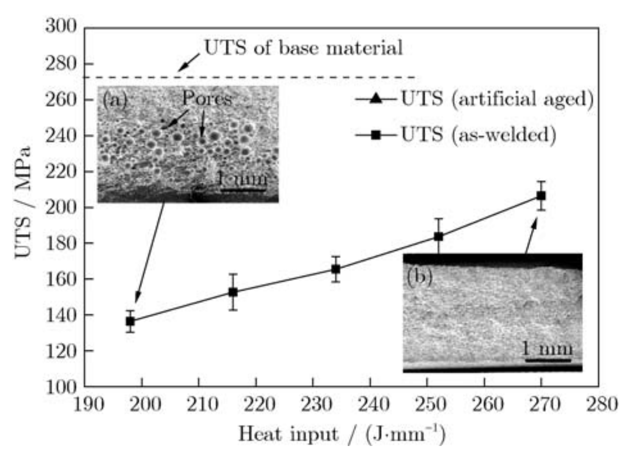

Fig. 7. Effects of heat input and post-weld aging on the UTS values of the TIG-welded joints: (a) low magnification fracture surface at the heat input of 198 J/mm, and (b) at the heat put of 270 J/mm.

protects the surface of the molten pool, whereas the back of the sample fails to be protected. Hence, air intrudes easily into the molten pool and results in the formation of pores in the welded seams. However, with the increase in heat input, the UTS values of the welded joints increase. The highest UTS value (206.4 MPa) is achieved at the heat input of 270 J/mm. This is because the relatively low cooling rate avoids the rapid solidification of the molten pool; hence, air has enough time to escape from the molten pool and then the porosities decrease (Fig. 7(b)).

With the increase in heat input, the UTS values of the welded joints after post-weld aging treatment improve from 142.7 to 240.6 MPa. The artificial aging treatment is found to be beneficial to enhance the tensile strength of the TIG-welded joints. For example, the UTS values of the artificially aged joints and as-welded joints are 240.6 and 206.4 MPa (L = 270 J/mm), respectively. This promotion is because the uniform distribution of precipitates resulted by the aging treatment enhances the resistance to indentation during the action of tensile loading. [17].

3.2.3. Fracture surfaces

SEM images of the typical tensile fracture surfaces of the BM and TIG-welded joints (L = 270 J/mm) are shown in Fig. 8. Almost all the welded joints are found to fracture within the FZ, where the hardness is lower compared with those of the HAZ and the BM. The displayed fractographs invariably consist of dimples, indicating that most of the tensile specimens fail in the ductile manner under the action of tensile loading. The fracture surface of the BM is characterized by more tearing fibers and ridges (Fig. 8(a)), indicating that intense plastic flow occurs in the test sample of the BM before it is fractured. The size of the dimples in the fracture surface section of the artificially aged joint is smaller than that in the fracture surface section of the as-welded joint (Figs. 8(b) and 8(c)). The dimple size exhibits a direct proportional relationship with strength and ductility (i.e., if the dimple size is finer, then the strength and ductility of the respective joint is higher and vice versa) [18]. Therefore, the artificially aged joints reveals higher UTS values compared with the as-welded joints (Fig. 7).

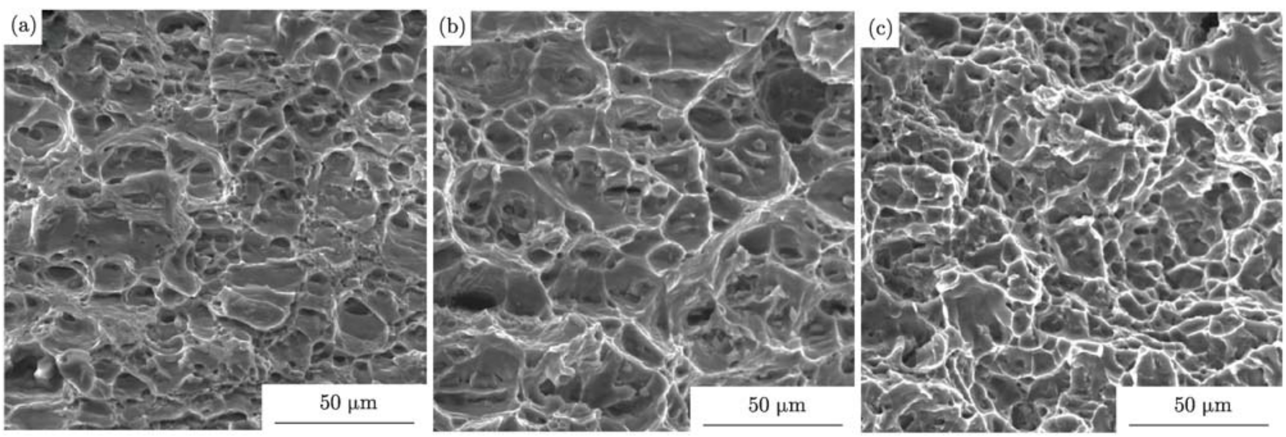

Fig. 8. Typical tensile fracture surfaces of the BM and the TIG-welded joints at the heat input of 270 J/mm: (a) BM; (b) as-welded; (c) post-welded aging.

4. Conclusions

In this article, the effects of post-weld aging treatment and heat input on the microstructures and mechanical properties of TIG-welded 6061-T6 aluminum alloy joints have been investigated. The main conclusions may be derived as follows.

(1) An increase in heat input results in increases in width of the HAZ and grain size of the FZ of the 6061-T6 TIG welding joints. No appreciable changes in grain size have been noticed after post-weld aging treatment.

(2) The hardness of the FZ is lower than those of the BM and HAZ. With an increase in heat input, the hardness values of the HAZ decrease, whereas the hardness values of the FZ decrease initially and then increase slightly. Post-weld aging treatment is beneficial to improve the hardness of the TIG-welded aluminum alloy joints.

(3) Partial penetration and pores present at low heat input and result in low UTS values of the welded joints. Post-weld aging treatment is found to increase the tensile strength of the TIG-welded 6061-T6 joints. Fracture surfaces of the welded joints are characterized by ductile fracture.

Acknowledgements

This research was financially supported by the Natural Science Foundation Project of Chongqing City (No.

cstc2012jjA50002).

References

[1] D. Maisonnette, M. Suery, D. Nelias, P. Chaudet, and T. Epicier, Effects of heat treatments on the microstructure and mechanical properties of a 6061 aluminium alloy, *Mater. Sci. Eng. A*, 528(2011), No. 6, p. 2718.

[2] D. Halil and G. Süleyman, The effects of aging on machinability of 6061 aluminium alloy, *Mater. Des.*, 30(2009), No. 5, p. 1480.

[3] M.I. Khan, *Welding Science and Technology*, New Age International, Lucknow, 2008, p. 42.

[4] M. Temmar, M. Hadji, and T. Sahraoui, Effect of post-weld aging treatment on mechanical properties of tungsten inert gas welded low thickness 7075 aluminium alloy joints, *Mater. Des.*, 32(2011), No. 6, p. 3532.

[5] V. Balasubramanian, V. Ravisankar, and G.M. Reddy, Effect of pulsed current and post weld aging treatment on tensile properties of argon arc welded high strength aluminum alloy, *Mater. Sci. Eng. A*, 459(2007), No. 1-2, p. 19.

[6] S. Malarvizhi and V. Balasubramanian, Effects of welding processes and post-weld aging treatment on fatigue behavior of AA2219 aluminum alloy joints, *J. Mater. Eng. Perform.*, 20(2011), No. 3, p. 359.

[7] S. Kou, *Welding Metallurgy*, 2nd Ed., John Wiley & Sons, New Jersey, 2003, p. 304.

[8] T. Oppenheim, S. Tewfic, T. Scheck, V. Klee, S. Lomeli, W. Dahir, P. Youngren, N. Aizpuru, R. Clark Jr., E.W. Lee, J. Ogren, and O.S. Es-Said, On the correlation of mechanical and physical properties of 6061-T6 and 7249-T76 aluminum alloys, *Eng. Fail. Anal.*, 14(2007), No. 1, p. 218.

[9] H. Agarwal, A.M. Gokhale, S. Graham, and M.F. Horstemeyer, Void growth in 6061-aluminum alloy under triaxial stress state, *Mater. Sci. Eng. A*, 341(2003), No. 1-2, p. 35.

[10] Z. Nikseresht, F. Karimzadeh, M.A. Golozar, and M. Heidarbeigy, Effect of heat treatment on microstructure and corrosion behavior of Al6061 alloy weldment, *Mater. Des.*, 31(2010), No. 5, p. 2643.

[11] J. Kupczyk, Application of significance tests in quantitative metallographic analysis of a C-Mn-B steel, *Mater. Charact.*, 57(2006), No. 3, p. 171.

[12] D. Min, J. Shen, S.H. Lai, and J. Chen, Effect of heat input on the microstructure and mechanical properties of tungsten inert gas arc butt-welded AZ61 magnesium alloy plates, *Mater. Charact.*, 60(2009), No. 12, p. 1583.

[13] S. Malarvizhi, K. Raghukandan, and N. Viswanathan, Effect of post weld aging treatment on tensile properties of electron beam welded AA2219 aluminum alloy, *Int. J. Adv. Manuf. Technol.*, 37(2008), No. 3-4, p. 294.

[14] T. Ma and G. den Ouden, Softening behaviour of Al-Zn-Mg alloys due to welding, *Mater. Sci. Eng. A*, 266(1999), No. 1-2, p. 198.

[15] T. Marlaud, A. Deschamps, F. Beley, W. Lefebvre, and B. Baroux, Evolution of precipitate microstructures during the retrogression and re-ageing heat treatment of an Al–Zn–Mg–Cu alloy, *Acta Mater.*, 58(2010), No. 14, p. 4814.

[16] M.R. Rezaei, M.R. Toroghinejad, and F. Ashrafizadeh, Effects of ARB and ageing processes on mechanical properties and microstructure of 6061 aluminum alloy, *J. Mater. Process. Technol.*, 211(2011), No. 6, p. 1184.

[17] A Sluzalec, *Theory of Thermomechanical Processes in Welding*, Springer, The Netherlands, 2005, p. 206.

[18] H. Aydın, A. Bayram, and I. Durgun, The effect of post-weld heat treatment on the mechanical properties of 2024-T4 friction stir-welded joints, *Mater. Des.*, 31(2010), No. 5, p. 2568.